

Technische Universität Berlin

Institute of Computer Engineering and Microelectronics

Dept. Computational Psychology

Prof. Dr. Marianne Maertens



The Effect of Low Luminance on the Perception of Transparency and Contrast

A thesis for obtaining the academic degree of
Bachelor of Science in the study of Information Systems Management
(Wirtschaftsinformatik)

submitted by

Sam Chamani

Matriculation number: 382485

Examiners: Prof. Dr. Marianne Maertens, Technische Universität Berlin
Prof. Dr. Felix Wichmann, Eberhard Karls Universität Tübingen

Supervisors: Prof. Dr. Marianne Maertens, Technische Universität Berlin
Dr. Guillermo Aguilar, Technische Universität Berlin

October 30, 2023

Statutory Declaration / Eidstattliche Erklärung

I hereby declare that I have created this work completely on my own and used no other sources or tools than the ones listed.

Hiermit erkläre ich, dass ich die vorliegende Arbeit selbstständig und eigenhändig sowie ohne unerlaubte fremde Hilfe und ausschließlich unter Verwendung der aufgeführten Quellen und Hilfsmittel angefertigt habe.



Berlin, October 30, 2023

Sam Chamani

Abstract

Previous work by Aguilar and Maertens (2022) suggested that the human observer judges perceived transparency and perceived contrast with the help of a common mechanism, that can be computationally captured as a logarithmic contrast. In their experiments, human observers compared the perceived transparency or the perceived contrast of several stimuli. The stimuli showed variegated checkerboards partially covered by transparent overlays, that varied in transmittance and luminance. The perceptual difference scales of these experiments were predicted well by contrast metrics based on the logarithm of the Michelson or Whittle contrast. However, their experiments only included stimuli with a minimum luminance of 60 cd/m^2 , thereby excluding the range in which logarithmic contrast metrics converge on one point. In this thesis, I used the same experimental method and procedure as Aguilar and Maertens (2022) to investigate the luminance range below 60 cd/m^2 and could reveal a systematic deviation in the predictions of the logarithmic contrast metrics. I used maximum likelihood conjoint measurement (MLCM) to generate perceptual scales for each observer and compared them with the contrast metrics evaluated in the previous study. Contrary to the predictions of the logarithmic contrast metrics, the perceptual scales do not appear to converge towards a single point as the luminance approaches 0 cd/m^2 .

Zusammenfassung

Die vorangehende Arbeit von Aguilar und Maertens (2022) deutet an, dass der menschliche Beobachter wahrgenommene Transparenz und wahrgenommenen Kontrast mit der Hilfe eines gemeinsamen Mechanismus beurteilt, welcher rechnerisch als logarithmischer Kontrast erfasst werden kann. In ihren Experimenten verglichen menschliche Beobachter die wahrgenommene Transparenz und den wahrgenommenen Kontrast vieler Stimuli. Die Stimuli stellten vielfarbige Schachbretter dar, welche jeweils teilweise von einer transparenten Ebene überdeckt wurden, die sich in Durchlässigkeit und Luminanz unterschied. Die Wahrnehmungsdifferenzskalen dieser Experimente wurden gut von Kontrastmetriken vorhergesagt, die auf dem Logarithmus des Michelson- oder Whittle-Kontrast basierten. Jedoch wurden nur Stimuli verwendet, in denen die transparente Ebene mindestens eine Luminanz von 60 cd/m^2 hatte, wodurch der Luminanzbereich, in dem die logarithmischen Kontrastmetriken auf einen Punkt führen, ausgeschlossen wurde. In dieser Abschlussarbeit habe ich die gleiche experimentelle Methode und Prozedur wie Aguilar und Maertens (2022) verwendet um den Luminanzbereich unter 60 cd/m^2 zu untersuchen und konnte eine systematische Abweichung in den Vorhersagen der logarithmischen Kontrastmetriken aufzeigen. Ich verwendete Maximum Likelihood Conjoint Measurement (MLCM) um für jeden Beobachter Wahrnehmungsskalen zu generieren und habe diese mit Kontrastmetriken, die in der vorangegangenen Arbeit evaluiert wurden, verglichen. Im Gegensatz zu den Vorhersagen der logarithmischen Kontrastmetriken scheinen die Wahrnehmungsskalen für eine Luminanz gegen 0 cd/m^2 sich nicht an einem Punkt zu sammeln.

Contents

| | | |
|----------|---|-----------|
| 1 | Introduction | 1 |
| 1.1 | Physical Transparency | 1 |
| 1.2 | Perceived Transparency | 2 |
| 1.3 | Metelli’s Episcotister Model | 4 |
| 1.4 | Related Work | 5 |
| 1.5 | Research Question | 8 |
| 2 | Method | 10 |
| 2.1 | Observer | 10 |
| 2.2 | Stimuli | 10 |
| 2.2.1 | Variegated Checkerboards | 11 |
| 2.2.2 | Cut-Out Stimuli | 12 |
| 2.2.3 | Stimuli Selection Process | 12 |
| 2.3 | Apparatus | 13 |
| 2.4 | Design and Procedure | 15 |
| 2.5 | Scale Estimation With Maximum Likelihood Conjoint Measurement | 15 |
| 3 | Results | 17 |
| 3.1 | Perceptual Scales | 17 |
| 3.2 | Contrast Metrics | 19 |
| 3.3 | Heatmaps | 20 |
| 4 | Discussion | 22 |
| 4.1 | Relation to Previous Work | 22 |

Contents

| | | |
|----------|-------------------------------------|-----------|
| 4.2 | Effects of Low Luminances | 23 |
| 5 | Conclusion | 26 |
| | References | 27 |
| | Appendix | 28 |
| 1 | Heatmaps | 29 |
| 2 | Observer Feedback Summary | 30 |

1 Introduction

In the context of vision research, transparency has two essential viewpoints: transparency can be examined as a physical attribute or as a perceptual phenomenon. In the forthcoming sections, I will outline these perspectives and discuss the episcotister model, a well-known physical model for transparency by Metelli (1970, 1985). As the episcotister model shares similar attributes with the stimuli used in the experiments of this thesis, I employ it to introduce the independent variables. Subsequently, I highlight discoveries of previous studies as well as how they are related to the objective of this thesis.

1.1 Physical Transparency

Robilotto and Zaidi (2004) define physical transparency as a filter medium property derived from the reflectivity and inner transmittance of the medium. Reflectivity is a physical property quantified as the ratio of radiant flux that is reflected on the front and back surfaces of a filter medium. The sum of all reflected radiant flux determines the reflectance of the medium. The inner transmittance of the filter medium is a property defining the ratio of radiant flux entering the medium's front surface and reaching the back surface. Correspondingly, the sum of all transmitted radiant flux determines the transmittance of the medium. [Figure 1.1](#) illustrates the path of radiant flux as it passes through a filter medium, but is also reflected on all surfaces.

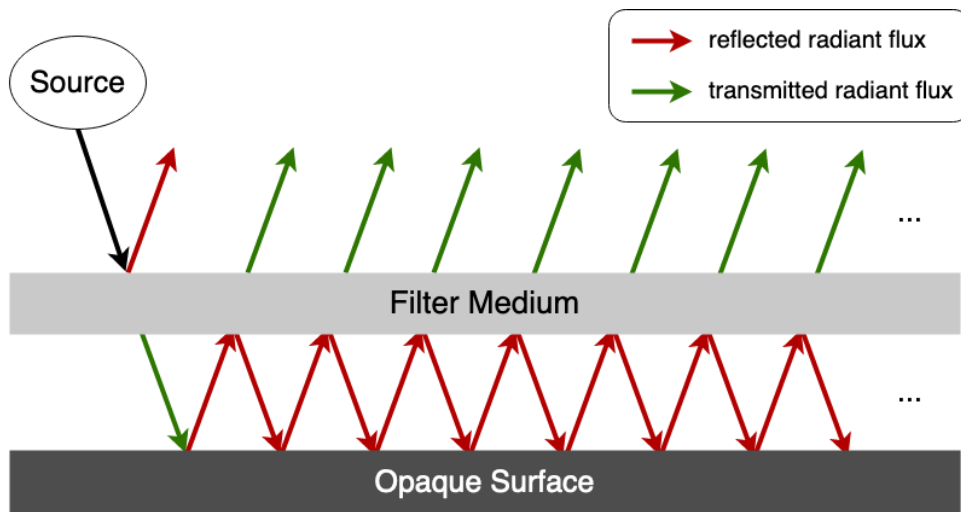


Figure 1.1: This figure is based on an illustration by Robilotto and Zaidi (2004) and shows the path of radiant flux as it passes through a transparent filter medium. When the flux initially reaches the front surface of the medium a part of the flux is reflected at the surface and another part passes through the medium. Subsequently, the transmitted flux reflects from the opaque surface and returns to the back surface of the filter. It then undergoes a series of reflections between the filter’s back surface and the opaque surface, occasionally passing through the medium when it reaches the back surface.

1.2 Perceived Transparency

Many researchers in the field of vision science studied the phenomenon of perceived transparency to address the fundamental question of how the human visual system decomposes the sensory input — a two-dimensional array of light intensities — into separate sources for the corresponding image data. In the case of transparency perception, the human observer seemingly sees one surface through another while perceiving reflected light from both surfaces separately. Regardless of the two-dimensional nature of the sensory input, the perceptual process allows the observer to perceive meaningful information about a three-dimensional environment (Aguilar & Maertens, 2022; Anderson et al., 2006; Singh & Anderson, 2002). However, Metelli (1970, 1974, 1985) has shown that perceived transparency does not rely on physical transparency. Instead, a stimulus must meet figural and chromatic conditions to be perceived as transparent. Figure 1.2 illustrates the effect of these conditions by showing three arrangements of the same four opaque geometric

1 Introduction

shapes. One of the arrangements meets all conditions while the other two violate one. The reflectances of the left and right rectangles are labeled as a and b , and the reflectances of the left and right semicircles are labeled as p and q . With these labeled shapes, we can establish the definitions of two chromatic conditions.

1. $a > b \Rightarrow p > q$ or $a < b \Rightarrow p < q$

If the left rectangle is brighter (or darker) than the right, then so is the left semicircle brighter (or darker) than the right one.

2. $|p - q| < |a - b|$

The difference between the reflectances of the semicircles has to be smaller than the difference between the reflectances of the rectangles.

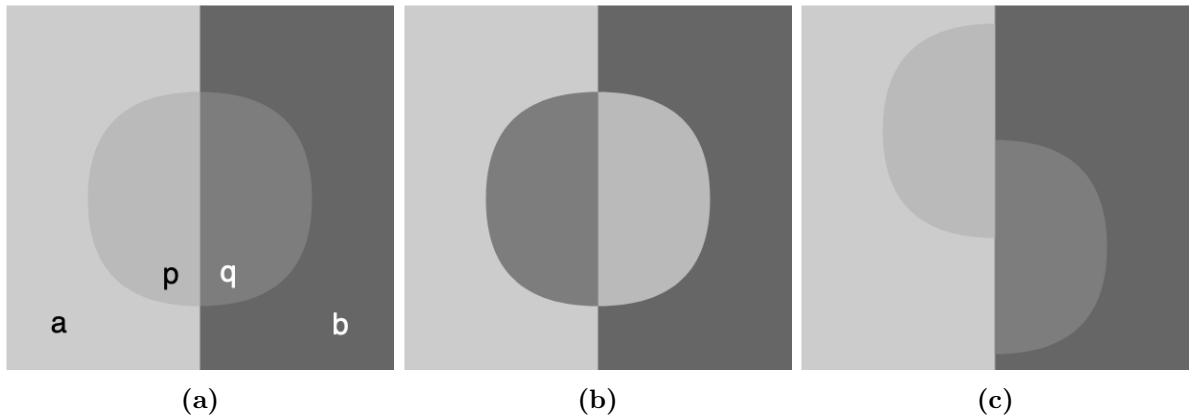


Figure 1.2: Three arrangements of the same four opaque geometric shapes based on the work of Metelli (1985). The reflectances of the left and right rectangles are labeled as a and b , and the reflectances of the left and right semicircles are labeled as p and q . (a) illustrates the case where the arrangement meets the figural and chromatic conditions of Metelli. (b) uses the same figural constellation as (a) but with the reflectances of the semicircles exchanged. This is an example where chromatic conditions are not fulfilled ($a > b$ but $p < q$). (c) displays an example of a breach of figural conditions: the shift of the semicircles causes the boundaries of the transparent layer to be aligned with the contour of the rectangles.

1.3 Metelli’s Episcotister Model

Metelli (1970) introduced a physical model for transparency known as the episcotister model. The episcotister is a rotating opaque disk with a cutout sector positioned in front of a background as illustrated in Figure 1.3. If the rotation speed is fast enough, the disk will appear as a transparent full circle similar to Figure 1.2a. The luminance reflected from the disk’s surface is denoted as τ . The size of the cutout sector is determined by $\alpha \in [0; 1]$, which represents the transmittance of the spinning disk. Aguilar and Maertens (2022) demonstrated that the degree of transparency perception does not solely depend on the transmittance α , but also on the luminance τ (see Figure 1.3). Talbot’s law can be used to predict the luminance of the transparent circle based on the background’s luminance, the luminance τ of the disk when opaque, and the transmittance α . For example, the luminance of q in Figure 1.2a can be calculated as follows:

$$q = \tau \cdot (1 - \alpha) + b \cdot \alpha \quad (1.1)$$

Incorporating the ideas of this model, I use various values for the transmittance α and the luminance τ to generate stimuli with different transparent layers.

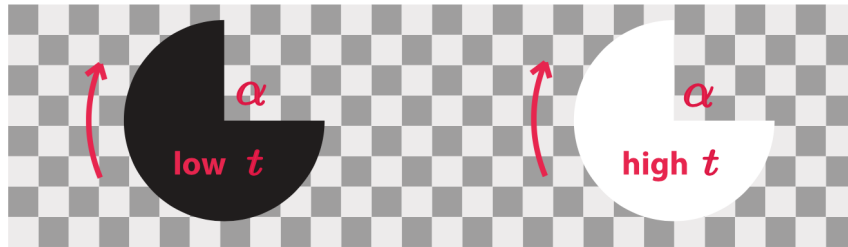


Figure 1.3: An illustration by Aguilar and Maertens (2022) showing two episcotisters with an equal transmittance $\alpha = 0.25$ and distinct reflectances for τ . The left episcotister has a dark surface and the right episcotister has a bright surface. When the episcotisters rotate at high speed, they appear as transparent full circles, but observers perceive the dark episcotister as more transparent.

1.4 Related Work

So far, no model can accurately predict the perceived transparency of a given image, but prior research suggests that the perception of transparency closely corresponds to the perception of contrast (Robilotto & Zaidi, 2004). Aguilar and Maertens (2022) investigated this matter by conducting two experiments involving human observers to identify their decision patterns for transparency and contrast perception using a perceptual difference scale. They then compared the accuracy of several contrast metrics in predicting the observers’ perceptual scales.

In the first experiment, observers were shown two identical variegated checkerboards that were partially covered by distinct transparent layers (see Figure 1.4a). Every trial employed a random checkerboard pattern and the transparent layers varied in reflectance and transmittance. When opaque, the transparent layer’s luminance had one of nine values ranging from 60 to 360 cd/m². In each trial, the observers judged which of the displayed stimuli appeared more transparent, hence comparing all combinations of the transparent layer’s reflectance transmittance with each other. The second experiment utilized the same procedure, but only the intersections of the transparent layers and the checkerboard’s top surfaces were visible, thereby removing cues to depth and transparency from the stimuli (see Figure 1.4b). Here, the observers had to decide which of the stimuli had a higher contrast.

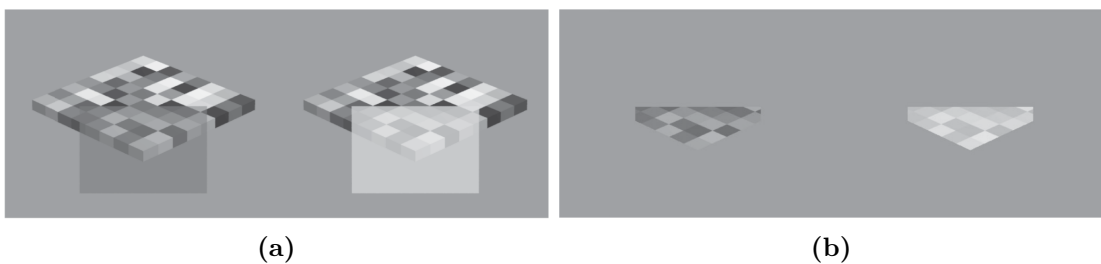


Figure 1.4: Example trials from the experiments of Aguilar and Maertens (2022). (a) showing a trial from the first experiment. Observers had to decide which stimulus appeared more transparent. (b) displaying the corresponding trial of the second experiment. The same checkerboard was used for the same comparison, but visual cues to depth and transparency were removed. The observers judged which of the stimuli had a higher contrast.

1 Introduction

In the following, I will introduce the contrast metrics used by Aguilar and Maertens (2022). Let l_i with $i \in \{1, 2, \dots, n\}$ represent one of the luminances in the transparent region, \bar{l} denote their arithmetic mean, and n denote the total number of distinct luminances in that region.

- The root mean square (RMS) contrast is defined as the standard deviation of luminance values relative to the global mean. This metric predicts perceived contrast to depend solely on the transmittance of the transparent layer and not on its luminance when it is opaque.

$$RMS = \sqrt{\frac{1}{n} \sum_{i=1}^n (l_i - \bar{l})^2} \quad (1.2)$$

- An alternative formulation of the root mean square contrast in which it is normalized relative to the mean luminance \bar{l} . Due to this normalization, the model's prediction is also affected by the transparent layer's luminance when it is opaque.

$$RMS_{norm} = \frac{RMS}{\hat{l}} = \frac{\sqrt{\frac{1}{n} \sum_{i=1}^n (l_i - \bar{l})^2}}{\bar{l}} \quad (1.3)$$

- The root mean square of the logarithm of the luminances. This alters the predictions of the root mean square similarly to its normalized version.

$$SDLG = \sqrt{\frac{1}{n} \sum_{i=1}^n (\log(l_i) - \overline{\log(l)})^2} \quad (1.4)$$

- Singh and Anderson (2002) showed that for simple stimuli, a ratio of contrasts effectively predicts perceived transparency. This metric relies only on the maximum and minimum values of the transparent region and the same region in plain view, whereas the other listed metrics use all luminance values in the transparent region.

$$\alpha_C = \frac{C_{TRANSP}}{C_{PLAIN}}, \text{ with } C = \frac{l_{max} - l_{min}}{l_{max} + l_{min}} \quad (1.5)$$

1 Introduction

The following metrics are space averages, and therefore, all cases where $i = j$ are excluded from the calculation.

- The space-averaged Michelson contrast

$$SAM = \frac{1}{n^2} \sum_{i=1}^n \sum_{j=1}^n \left| \frac{l_i - l_j}{l_i + l_j} \right| \quad (1.6)$$

- The space-averaged logarithm of the Michelson contrast (SAMLG). This metric accurately predicted the perceptual scales from the experiments of Aguilar and Maertens (2022) with Pearson's correlation coefficient r of 0.99 in the first experiment and 0.98 in the second.

$$SAMLG = \frac{1}{n^2} \sum_{i=1}^n \sum_{j=1}^n \log \left| \frac{l_i - l_j}{l_i + l_j} \right| \quad (1.7)$$

- The space-averaged Whittle contrast.

$$SAW = \frac{1}{n^2} \sum_{i=1}^n \sum_{j=1}^n \left| \frac{l_i - l_j}{\min(l_i, l_j)} \right| \quad (1.8)$$

- The space-averaged logarithm of the Whittle contrast (SAWLG). This metric, too, predicted the perceptual scales accurately with Pearson's correlation coefficient r of 0.99 in both experiments.

$$SAWLG = \frac{1}{n^2} \sum_{i=1}^n \sum_{j=1}^n \log \left| \frac{l_i - l_j}{\min(l_i, l_j)} \right| \quad (1.9)$$

Figure 1.5 presents a graphical representation of these metrics' predictions based on the transmittance (α) of the transparent layer and its luminance when it is opaque (τ). Given α , τ , and the luminances of the background surface, the luminance values in the transparent region can be calculated using Talbot's law (see Equation 1.1).

1.5 Research Question

As demonstrated by Aguilar and Maertens (2022), the root mean square does not accurately predict transparency perception, as the model suggests that the degree of perceived transparency is unaffected by the luminance τ of the transparent layer. However, the other contrast metrics converge to a single point as τ approaches 0 cd/m^2 , which means that for the limiting case of $\tau = 0$, transparency or contrast is perceived as equal for all transmittances α (compare Figure 1.5). This is at odds with the intuitive assumption that for any luminance τ the stimulus with the higher transmittance α will be perceived as more transparent.

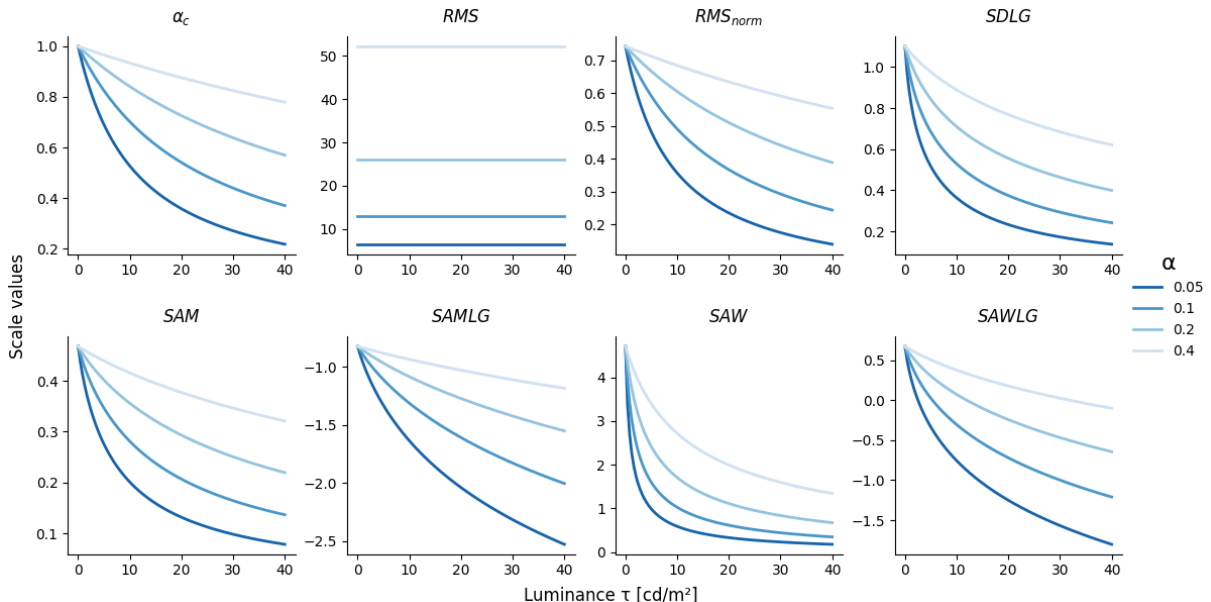


Figure 1.5: A graphical representation of the equations 1.2 to 1.9. The x-axis corresponds to the luminance of the transparent layer when it is opaque. The y-axis represents the perceptual scale which, in this case, simply refers to the range of the metric. The graphs employ different colors to distinguish the different transmittances α . I calculated all luminances required for these metrics using Talbot’s law (Equation 1.1) and the 13 possible luminance values of the checkerboard checks.

The contrast metrics based on the logarithm of the Whittle and Michelson contrast (see equations 1.9 and 1.7) achieved high accuracy in predicting the perceptual scales of the experiments conducted by Aguilar and Maertens (2022), but the lowest luminance value

1 Introduction

for τ was 60 cd/m^2 . Hence, the question of whether these contrast metrics can predict the perceived transparency for low luminances remains open and serves as the objective of this thesis. I investigate if human observers can distinguish differences in transparency as accurately in the low luminance range as in the range above 60 cd/m^2 . From this objective, I derive the following hypothesis:

If the contrast metrics predict perceived transparency as accurately for low luminances as for high luminances, then the pattern of the perceptual scales must align with the pattern of the predictions.

2 Method

I use the same experimental method, procedure, and type of stimuli as Aguilar and Maertens (2022) but employ lower values for the luminance τ of the transparent layer. In the following sections, I briefly introduce the human observers. Next, I will present the stimuli and describe the selection process. I will then list the equipment used and explain the design of the experiments. Finally, I introduce the method of maximum likelihood conjoint measurement, which I employed for scale estimation (Knoblauch & Maloney, 2012).

2.1 Observer

Three observers participated in the experiments. GA is one of the authors from the work of Aguilar and Maertens (2022), SN is a volunteer who served as a naive observer, and SC is me. The observers received instructions on how to interact with the gear used in the experiments and a brief explanation of the given tasks.

2.2 Stimuli

I generated variegated checkerboards and cut-out stimuli based on the work of Aguilar and Maertens (2022).

2.2.1 Variegated Checkerboards

I used povray (Persistence of Vision Raytracer Pty. Ltd., Williamstown, Victoria, Australia, 2004) to generate square variegated checkerboards with 64 checks. Each check had one out of 13 possible reflectances with a luminance ranging from 12 to 412 cd/m^2 . I randomized the assignment of reflectances to checks, however, two adjacent checks could not have the same reflectance. The configuration of the camera perspective and light source remained constant and created a 3D impression. I placed a transparent rectangle in front of the checkerboard, partially covering it. The appearance of the transparent rectangle was determined by the transmittance α and luminance τ . The background was consistent for all stimuli with a luminance of 133 cd/m^2 (see [Figure 2.1](#)). I modified the

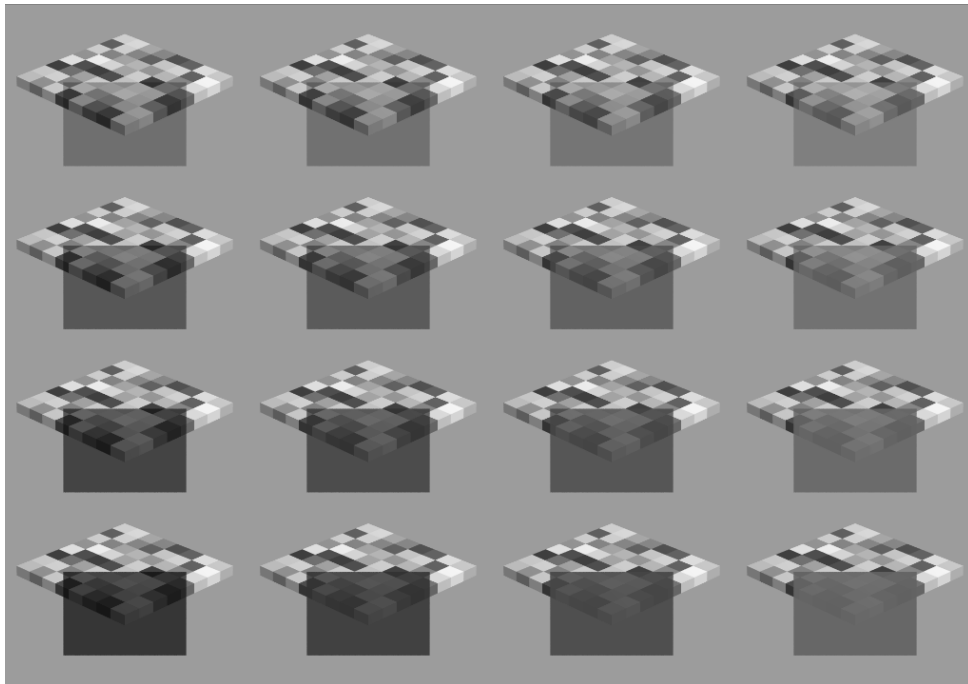


Figure 2.1: An example checkerboard pattern with all transparent layers used in the experiment. The stimuli are arranged based on the transmittance α (rows) and luminance τ (columns) of the transparent rectangle. The rows are sorted from top to bottom with the α values 0.4, 0.2, 0.1, 0.05. The columns are sorted from left to right with τ values 2, 8, 16, 41 cd/m^2 .

output of the rendering process to be 16-bit PNG files, departing from the 8-bit PNG files employed by Aguilar and Maertens (2022). This adjustment successfully addressed

an issue where extra edges appeared on some of the checks due to povray's challenges in rendering dark transparent overlays.

2.2.2 Cut-Out Stimuli

For the stimuli of the second experiment, I reused the variegated checkerboard from the first experiment. I applied a mask that removed depth and transparency cues displaying only the intersection of the checkerboard's top surface and the transparent rectangle. The background luminance remained unchanged (see [Figure 2.2](#)).

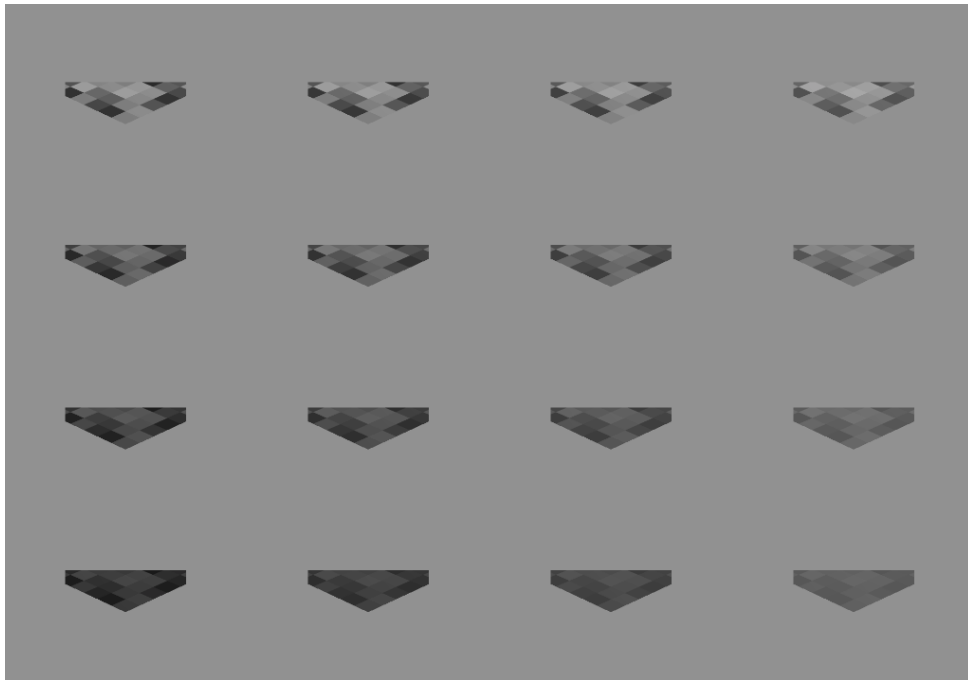


Figure 2.2: The same stimuli as in [Figure 2.1](#), but with a cut-out mask applied to show only the intersection of the checkerboard's top surface and the transparent rectangle.

2.2.3 Stimuli Selection Process

The transmittance values used to generate the stimuli of my experiments (?? and ??) were consistent with those employed by Aguilar and Maertens (2022): 0.05, 0.1, 0.2, or 0.4. The relevant range of the luminance τ spans from 0 to 60 cd/m². To select adequate

2 Method

luminances, I generated multiple sets of stimuli. I compared these sets using a custom exploration tool, which allowed me to navigate through them, adjusting the number of τ values, the spacing of the values, and the maximum luminance. Figure 2.3 provides an example view of this mode where the transmittance α was set to 0, displaying the transparent rectangle in an opaque state. The transmittance displayed in a given view could be increased or decreased, and a cut-out mask could be applied, too. As a result of this procedure, I selected the following four values the luminance τ : 2, 8, 16, and 41 cd/m^2 . 2 cd/m^2 is the lowest luminance that could be displayed on the monitor for the experiments. The values in between were chosen due to the perceptually equal spacing in lightness.

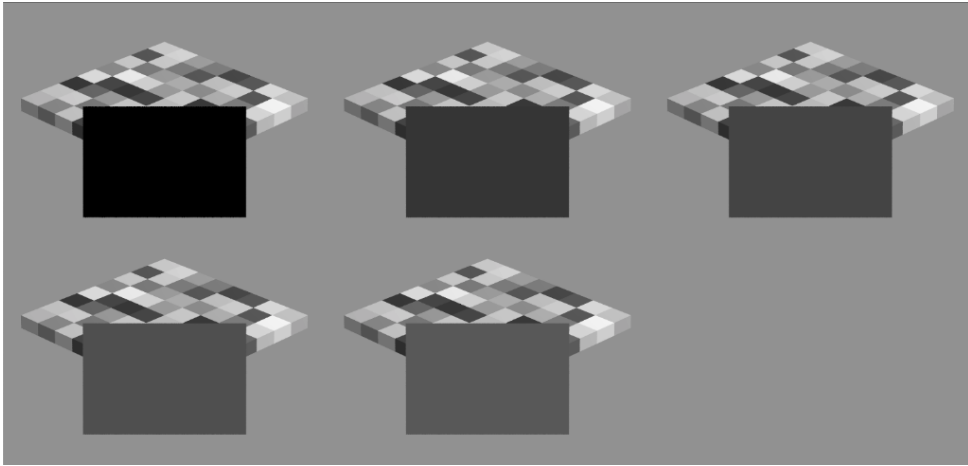


Figure 2.3: An example screen of the exploration mode. A set of stimuli with a fixed transmittance α was presented at once. Pressing the up or down button changed the transmittance and eventually the stimuli type (variegated checkerboards or cut-out stimuli). Pressing the left or right button changed the set of stimuli. The sets differed in the number of values for τ (4-9 values), the spacing of the values, and the highest luminance.

2.3 Apparatus

The experiments were conducted in the same facility as the experiments of Aguilar and Maertens (2022). The observers were watching a screen from a distance of 130 cm inside a dark experimental cabin. The following is a list of the equipment used in the experiments:

2 Method

- 21-in. Siemens SMM2106LS monitor (400×300 mm, $1,024 \times 768$ px, 130 Hz) for stimuli presentation.
- Minolta LS-100 photometer (Konica Minolta, Tokyo, Japan) for the calibration of the monitor and measurement of luminances.
- DataPixx toolbox (Vpixx Technologies, Inc., Saint- Bruno, QC, Canada) for control of the presentation.
- ResponsePixx button-box (VPixxTechnologies, Inc.) for response registration.

I switched the monitor on at least 30 minutes before each session, ensuring it had enough time for its auto-calibration. The authors of the previous experiments provided a table for the linearization of the monitor’s luminance response, based on the measurement of the monitor’s gamma function. The τ values mentioned in [subsection 2.2.3](#) were directly measured on the monitor screen. However, the estimated luminance values were slightly different since the luminance that can be produced is restricted by the monitor’s luminance response. Additionally, since povray uses a particular unit to specify reflectance values, I applied linear regression to calculate the luminance estimations. [Table 2.1](#) lists the mapping of the povray input values, the estimated luminances, and the measured luminances. For the presentation, I utilized custom software¹ to implement the specific components and Python scripts needed for my experiments.

| Povray reflectance value | Estimated luminance (cd/m ²) | Measured luminance (cd/m ²) |
|--------------------------|--|---|
| 0 | 0 | 2 |
| 0.10554 | 5.43 | 8 |
| 0.28649 | 14.74 | 16 |
| 0.77766 | 40 | 41 |

Table 2.1: The input reflectance values for povray (left column), the estimated luminance values to which the povray values are mapped (middle column), and the luminances measured on the experiment monitor screen (right column).

¹HRL: High Resolution Luminance – a library used for the experiments’ implementation. <http://github.com/computational-psychology/hrl>

2.4 Design and Procedure

The purpose of the experiments was to estimate perceptual differences for transparency and contrast at low luminance settings of the transparent medium using maximum likelihood conjoint measurement (Knoblauch & Maloney, 2012) and paired comparisons. I conducted a separate experiment for each type of stimulus. Both experiments had the same procedure: In each trial, two stimuli were presented side by side, and the observer had to select one stimulus based on the given task of the experiment. In Experiment 1, the task was to select the checkerboard in which the rectangle layer was perceived as more transparent. In Experiment 2, the observer judged which cut-out stimulus had a higher perceived contrast (compare Figure 1.4). There was no time limit for the trials. I generated a new random checkerboard pattern for each trial. Hence, the checkerboard patterns used by the stimuli of the same trial were identical. I also randomized the order of the trials and the position of the stimuli (left or right). Pressing the left or right button of the response box selected the corresponding left or right stimulus. Each experiment comprised 120 unique comparisons, repeated 10 times in distinct blocks, totaling 2400 trials per observer. The trials and stimuli within the blocks previously described randomization steps and assisted observers in tracking their progress. Observers were free to take breaks whenever needed. I have scheduled around two to three one-hour sessions for each observer. The order of the experiments was fixed, with observers first completing Experiment 1 and then Experiment 2.

2.5 Scale Estimation With Maximum Likelihood Conjoint Measurement

Using maximum likelihood conjoint measurement (MLCM) (Knoblauch & Maloney, 2012), it is possible to estimate scales that assess the effect of at least two physical dimensions on perceptual differences. In the experiments conducted in the scope of this thesis, the phys-

2 Method

ical dimensions are the luminance and transmittance of the transparent layer. The scale represents the perceptual difference in transparency (Experiment 1) or contrast (Experiment 2). MLCM is a version of conjoint measurement that allows for non-deterministic observer judgments. This means that decisions over the same parameter combination may vary across multiple iterations. To calculate the perceptual scales for each observer and experiment, I used the same implementation as Aguilar and Maertens (2022), available for the R programming language. This implementation provides three conjoint measurement models to fit the observer data (Knoblauch et al., 2022). Following the approach of Aguilar and Maertens (2022), I used the full model with a positive convergence tolerance ϵ set to 0.0001 to control the fit.

3 Results

To provide a comprehensive view of the experiment results, I utilize two visualizations: perceptual scales derived through MLCM and, as a complementary approach, heatmaps for a closer visualization of the raw data. I begin with the presentation of the perceptual scales for each observer and experiment (Figure 3.1), followed by the evaluation results for all metrics (Table 3.1) and the comparison of the most accurate contrast metric with the perceptual scales (Figure 3.2). Lastly, I illustrate certain and uncertain decisions of the observers in heatmaps (Figure 3.3).

3.1 Perceptual Scales

The differences in perceived transparency and contrast across the 16 combinations of transmittance and luminance can be deduced from the perceptual scales in Figure 3.1. The perceptual scales in Figure 3.1a reflect differences in perceived transparency, while scales in Figure 3.1b represent perceived contrast. All figures share the same x-axis, depicting the luminance (τ) of the transparent medium when it is opaque, spanning from 0 to 41 cd/m^2 . However, the scales on the y-axis differ among the observers, with the maximum scale value inversely reflecting their decision noise levels (a higher maximum indicates less decision noise). Distinct colors assigned to the data points correspond to a specific transmittance α . Data points of the same α are then connected to visually depict perceptual scale patterns for each observer. Vertical lines positioned at each data point denote error bars, which represent the 95% confidence intervals. Consistent with

3 Results

prior studies (Aguilar & Maertens, 2022; Robilotto & Zaidi, 2004), the perceptual scales indicate, that for each transmittance α , the stimuli with lower luminance τ were perceived as more transparent or richer in contrast than those with higher luminance. On the other hand, stimuli with a higher transmittance α were perceived as more transparent or richer in contrast for each luminance τ . Notably, The scales do not converge to a single point as luminance approaches 0 cd/m^2 .

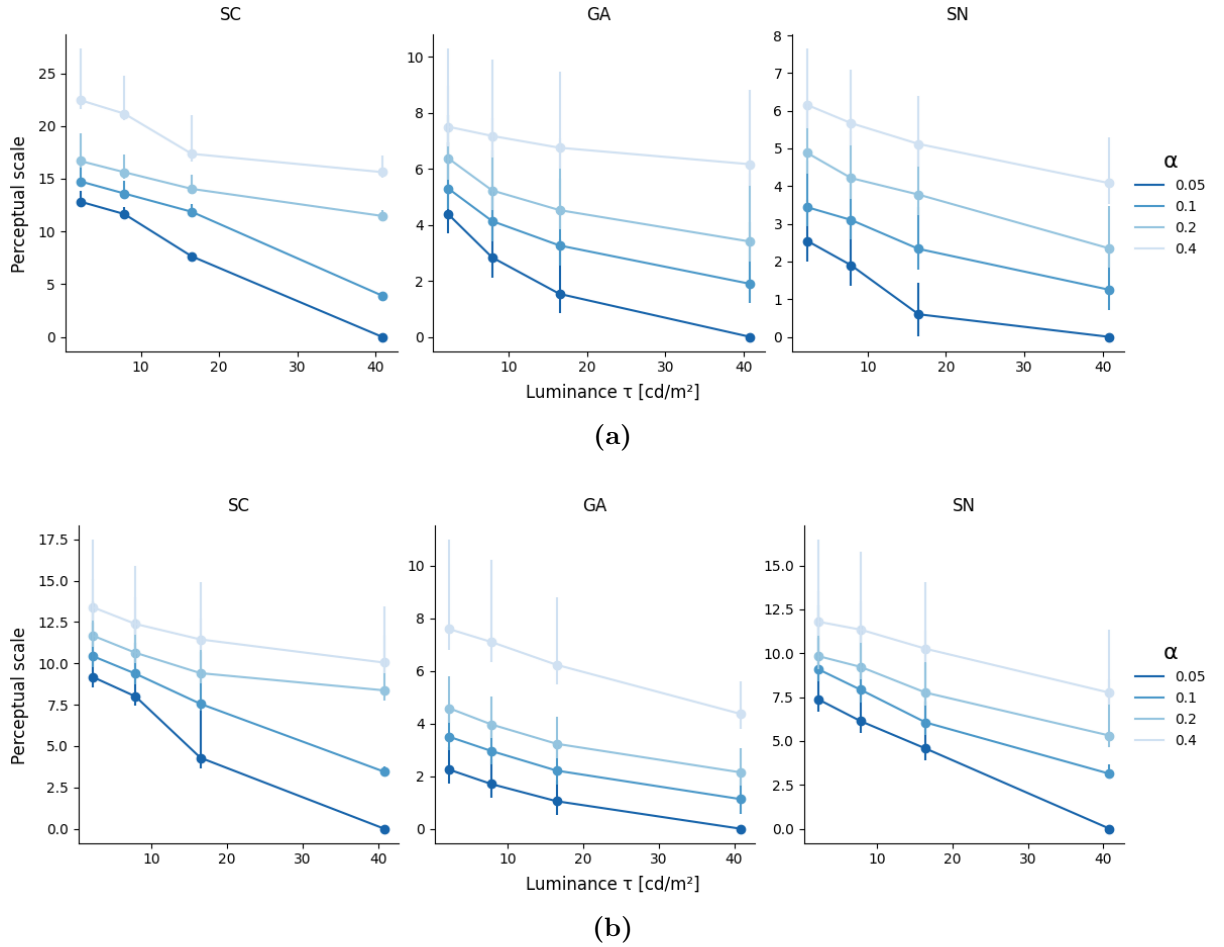


Figure 3.1: The perceptual scales of the observers. (a) Experiment 1 with perceived transparency. (b) Experiment 2 with perceived contrast. The x-axis represents the opaque luminance τ of the transparent layer, colored lines indicate the transmittance α , and vertical lines are 95% confidence intervals. Each figure includes 16 data points, representing different τ and α combinations, used for the stimuli.

3.2 Contrast Metrics

| Contrast metric | Exp. | SSE | | r avg. |
|-----------------|------|-------|-----------------|----------|
| | | Avg. | Range | |
| α_c | 1 | 22.92 | [6.25, 55.74] | 0.94 |
| | 2 | 12.97 | [8.41, 19.11] | 0.93 |
| RMS | 1 | 88.87 | [14.97, 227.39] | 0.79 |
| | 2 | 65.46 | [15.77, 102.79] | 0.74 |
| RMS_{norm} | 1 | 23.71 | [6.03, 58.7] | 0.94 |
| | 2 | 13.47 | [8.74, 18.06] | 0.93 |
| $SDLG$ | 1 | 28.38 | [5.63, 72.71] | 0.94 |
| | 2 | 17.11 | [12.3, 25.04] | 0.93 |
| SAM | 1 | 24.34 | [5.85, 61.31] | 0.94 |
| | 2 | 14.02 | [9.1, 16.65] | 0.93 |
| $SAMLG$ | 1 | 22.26 | [8.06, 50.02] | 0.93 |
| | 2 | 12.63 | [6.57, 22.85] | 0.93 |
| SAW | 1 | 50.64 | [8.95, 128.48] | 0.88 |
| | 2 | 33.16 | [14.15, 54.82] | 0.87 |
| $SAWLG$ | 1 | 19.51 | [5.9, 46.11] | 0.95 |
| | 2 | 10.98 | [6.1, 18.36] | 0.94 |

Table 3.1: Comparison between the predictions of the contrast metrics and the perceptual scales, following the evaluation procedure from Aguilar and Maertens (2022). Averages of the sum of squared errors (SSE Avg.), the ranges of SSE (SSE Range), and the average Pearson’s correlation coefficients (r avg.) calculated across all observers for each contrast metric and experiment.

I scaled the contrast metrics’ predictions (compare Figure 1.5) to match each observer’s individual scale range employing linear transformation. Subsequently, I computed the sum of squared errors and Pearson’s correlation coefficient r between each prediction and the respective observer’s perceptual scale. The averages of the sum of squared errors and Pearson’s correlation coefficient r , as well as the range of the sum of squared errors across all observers, are listed in Table 3.1. None of the contrast metrics demonstrated a significantly better fit over the others. While the contrast metric based on the logarithm

3 Results

of the Whittle contrast (SAWLG) performed slightly better than the other metrics, it did not yield a satisfactory fit (see [Figure 3.2](#)).

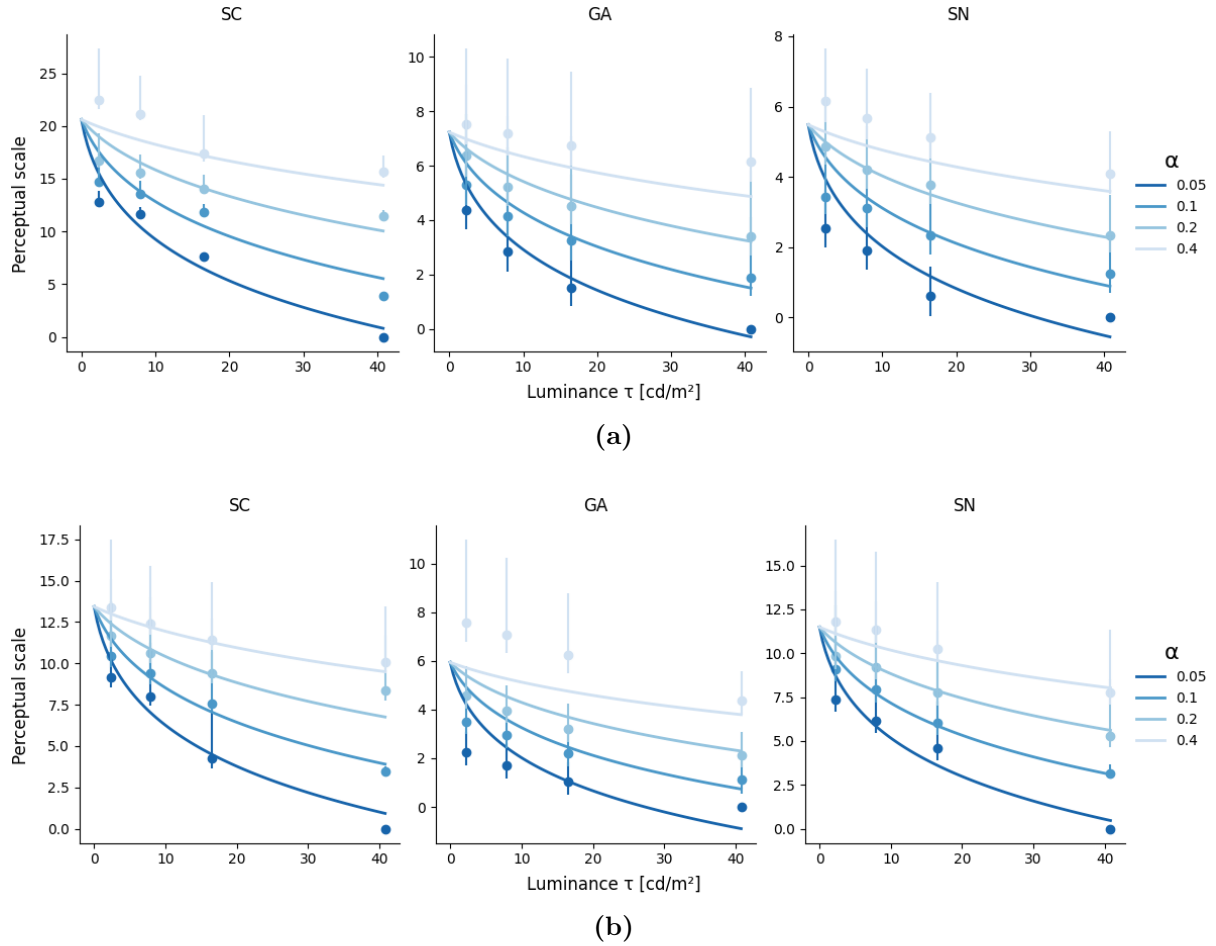


Figure 3.2: The perceptual scales of the observers (represented by dots with error bars) and the predictions of SAWLG, individually scaled to match the range of the corresponding perceptual scale. Similar to [Figure 3.1](#), (a) corresponds to the first experiment and (b) to the second.

3.3 Heatmaps

Alongside the perceptual scales, I used heatmaps to visualize observer responses, offering a representation that closely resembles raw data and emphasizing challenging comparisons for the observers. [Figure 3.3](#) displays heatmaps for observer SC. These heatmaps are composed of colored boxes, with each box representing the relative frequency of selecting

3 Results

Stimulus 1 based on its transmittance α and luminance τ , depicted on the y-axis, in comparison to α and τ of Stimulus 2, which is represented on the x-axis. The level of redness in each box corresponds to the observer's uncertainty in their decision-making. Observers less familiar with the stimuli had a higher occurrence of red boxes. Next to the diagonal, black triangular patterns emerged, signifying that for consistent τ values, decisions leaned towards the stimulus with a higher α , aligning with the observations detailed in [section 3.1](#).

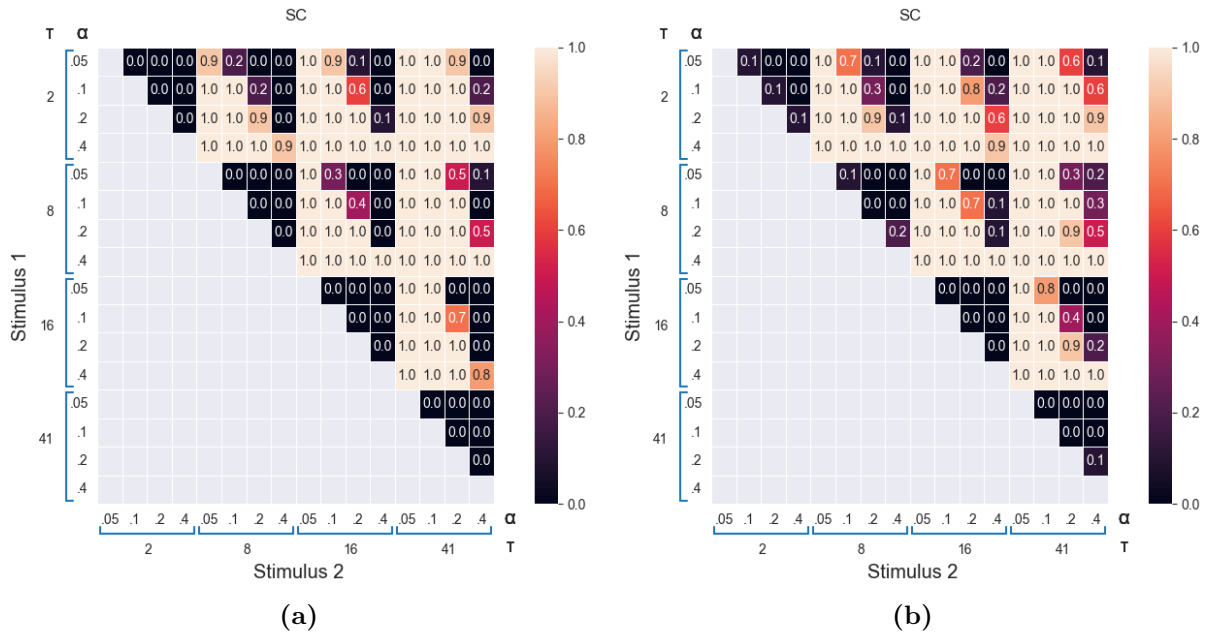


Figure 3.3: Heatmaps of Experiment 1 (a) and 2 (b) for observer SC reflect judgments for each comparison of transmittance α and luminance τ combination. Box values represent the relative frequency of choosing Stimulus 1, with red boxes denoting challenging comparisons. Heatmaps for all observers can be found in [Appendix 1](#).

4 Discussion

I examined whether human observers could distinguish stimuli when the luminance of the transparent layer was low. Furthermore, I assessed the accuracy of several contrast metrics in predicting the perceptual scales of observers for the tested luminance range. In the subsequent sections, I will discuss my findings, establish connections with prior research, and draw conclusions regarding the effects observed across the tested luminance values.

4.1 Relation to Previous Work

While the space-averaged contrast metrics based on the logarithm of Michelson or Whittle (SAMLG, SAWLG) were found to be the most suitable for capturing perceptual scales of the experiments by Aguilar and Maertens (2022), they did not yield similar results for the perceptual scales of the experiments conducted for my thesis. The perceptual scale patterns do not align with the predictions of the contrast metrics. It appears that, for the tested values, a linear function may be a more suitable choice for approximating perceptual scales compared to logarithmic functions. The contrast metric predictions based on the logarithm of Whittle (SAWLG) exhibited the smallest average sum of squared errors. However, they systematically deviated from the perceptual scales of all observers and experiments. Specifically, the predictions were consistently below the data points with a transmittance of $\alpha = 0.4$ and for luminance values below 8 cd/m^2 , the predictions' slope increased, leading to inaccurate predictions for $\alpha = 0.05$ and $\tau = 2 \text{ cd/m}^2$ (see

Figure 3.2 for comparison). The evaluation reveals that the contrast metrics do not effectively capture perceived transparency or contrast for the tested values. Nonetheless, the perceptual scale patterns in both experiments closely resemble each other, in line with previous studies suggesting a shared mechanism for judging perceived transparency and contrast (Aguilar & Maertens, 2022; Robilotto & Zaidi, 2004).

4.2 Effects of Low Luminances

Highlighted areas in Figure 4.1 represent comparisons in which both stimuli share the same luminance τ . In these instances, observers successfully differentiated transparencies and contrasts based on the transmittance α . The scales do not exhibit signs of converging at a single point. In contrast to the converging predictions of the contrast metrics, the patterns of the perceptual scales indicate that transparency perception for zero-reflectance transparencies is not independent of the transmittance.

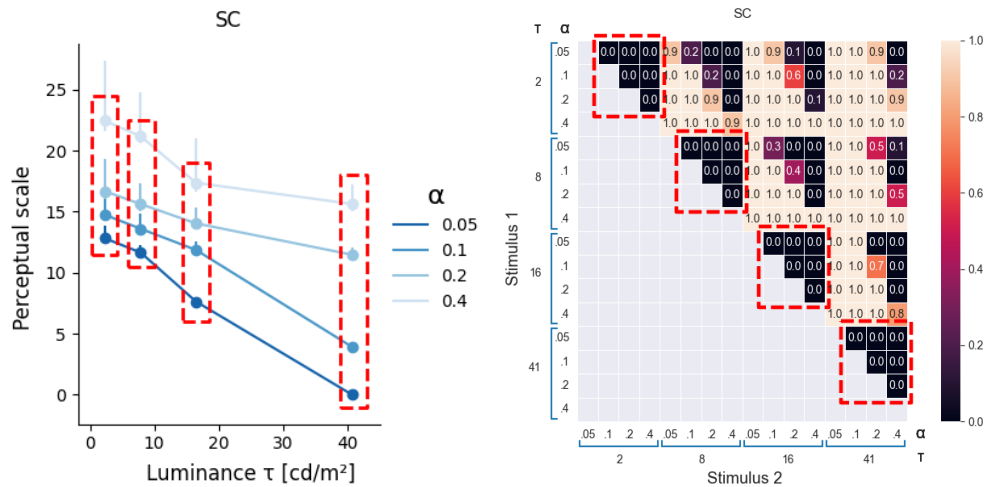


Figure 4.1: Perceptual scale and heatmap of observer SC in Experiment 1. Marked areas demonstrate the observer’s ability to distinguish transparency based on transmittance α , regardless of shared luminance τ .

The perceptual scales indicate that as the luminance of the transparent medium increases, the perception of both transparency and contrast decreases. Aguilar and Maertens (2022) characterized this perceptual phenomenon as a trade-off between the luminance and the

4 Discussion

transmittance of the transparent medium. Some comparisons, where observers couldn't consistently select the same stimulus due to no perceived difference in transparency or contrast, often resembled instances of this effect (as seen in the example provided in Figure 4.2).

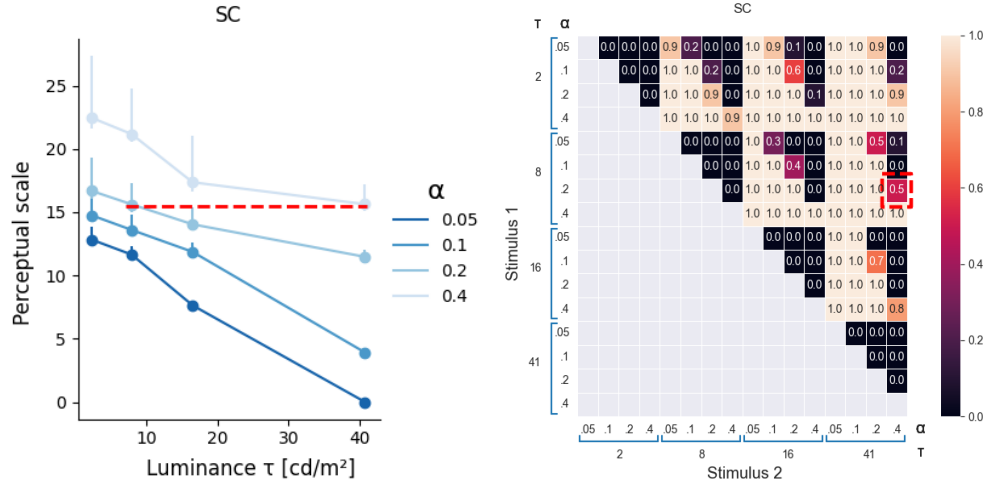


Figure 4.2: Perceptual scale and heatmap of observer SC in Experiment 1. The highlighted line represents a comparison where the observer did not perceive one stimulus as more transparent than the other. This example pertains the comparison between $\alpha = 0.2, \tau = 8 \text{ cd/m}^2$ and $\alpha = 0.4, \tau = 41 \text{ cd/m}^2$.

I included another example for this trade-off in Figure 4.3. In this case, observers tended to perceive higher transparency for the stimulus with the darker transparent layer, despite its lower transmittance. This confirms the persistence of this effect for the values tested within the scope of this thesis.

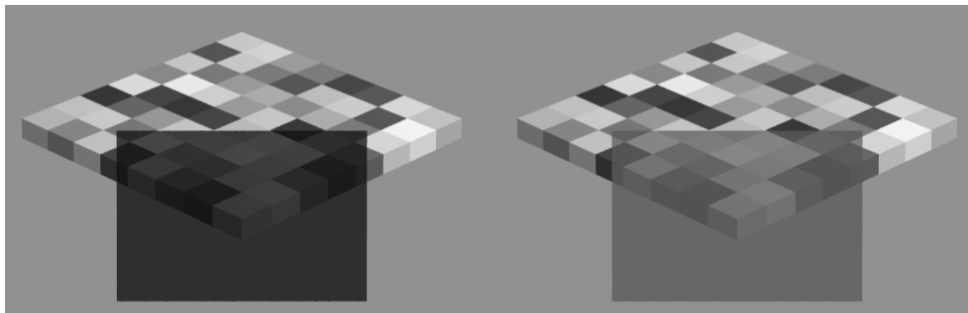


Figure 4.3: Example trial where a dark transparent layer was perceived as more transparent despite a lower transmittance α . The left stimulus has the values $\alpha = 0.05$ and $\tau = 2 \text{ cd/m}^2$. The right stimulus has the values $\alpha = 0.2$ and $\tau = 41 \text{ cd/m}^2$.

4 Discussion

The observers GA and SC commented on a somehow deviating appearance of dark transparent layers (see summarized observer feedback in [Appendix 2](#)). While the perceived transparency seems to appear hazy when the luminance is high, it becomes clearer as the luminance decreases. Based on this assumption, the transparency may reach maximum clarity as the luminance approaches 0 cd/m^2 .

5 Conclusion

I employed the experimental methodology of Aguilar and Maertens (2022) to investigate if observers can distinguish stimuli with low-luminance transparencies. Utilizing the data from the experiments, I generated perceptual scales for perceived transparency and contrast using MLCM. Despite predictions from several contrast metrics suggesting convergence on a single point as luminance approaches 0 cd/m^2 , my findings indicate that this is not the case. Observers consistently distinguished the transparency and contrast of stimuli with the same luminance.

In conclusion, none of the tested contrast metrics provided accurate predictions within the scope of this thesis. Additionally, I confirmed the significant impact of luminance on perceived transparency and contrast, and observed similarities in the perceptual scales between experiments, suggesting a common underlying mechanism for judging perceived transparency and contrast.

References

- Aguilar, G., & Maertens, M. (2022). Conjoint measurement of perceived transparency and perceived contrast in variegated checkerboards. *Journal of Vision*, *22*(2), 2–2. <https://doi.org/10.1167/jov.22.2.2>
- Anderson, B. L., Singh, M., & Meng, J. (2006). The perceived transmittance of inhomogeneous surfaces and media. *Vision Research*, *46*(12), 1982–1995. <https://doi.org/https://doi.org/10.1016/j.visres.2005.11.024>
- Knoblauch, K., Maloney, L. T., & Aguilar, G. (2022). *Maximum likelihood conjoint measurement* [Documentation of the MLCM package for the R programming language]. <https://cran.r-project.org/web/packages/MLCM/MLCM.pdf>
- Knoblauch, K., & Maloney, L. T. (2012). Maximum likelihood conjoint measurement. In *Modeling psychophysical data in r* (pp. 229–256). Springer New York. https://doi.org/10.1007/978-1-4614-4475-6_8
- Metelli, F. (1970). An algebraic development of the theory of perceptual transparency [PMID: 5416869]. *Ergonomics*, *13*(1), 59–66. <https://doi.org/10.1080/00140137008931118>
- Metelli, F. (1974). The perception of transparency.
- Metelli, F. (1985). Stimulation and perception of transparency. *Psychological Research*, *47*(4), 185–202. <https://doi.org/10.1007/BF00309446>
- Robilotto, R., & Zaidi, Q. (2004). Perceived transparency of neutral density filters across dissimilar backgrounds. *Journal of Vision*, *4*(3), 5–5. <https://doi.org/10.1167/4.3.5>
- Singh, M., & Anderson, B. (2002). Toward a perceptual theory of transparency. *Psychological review*, *109*, 492–519. <https://doi.org/10.1037/0033-295X.109.3.492>

Appendix

1 Heatmaps

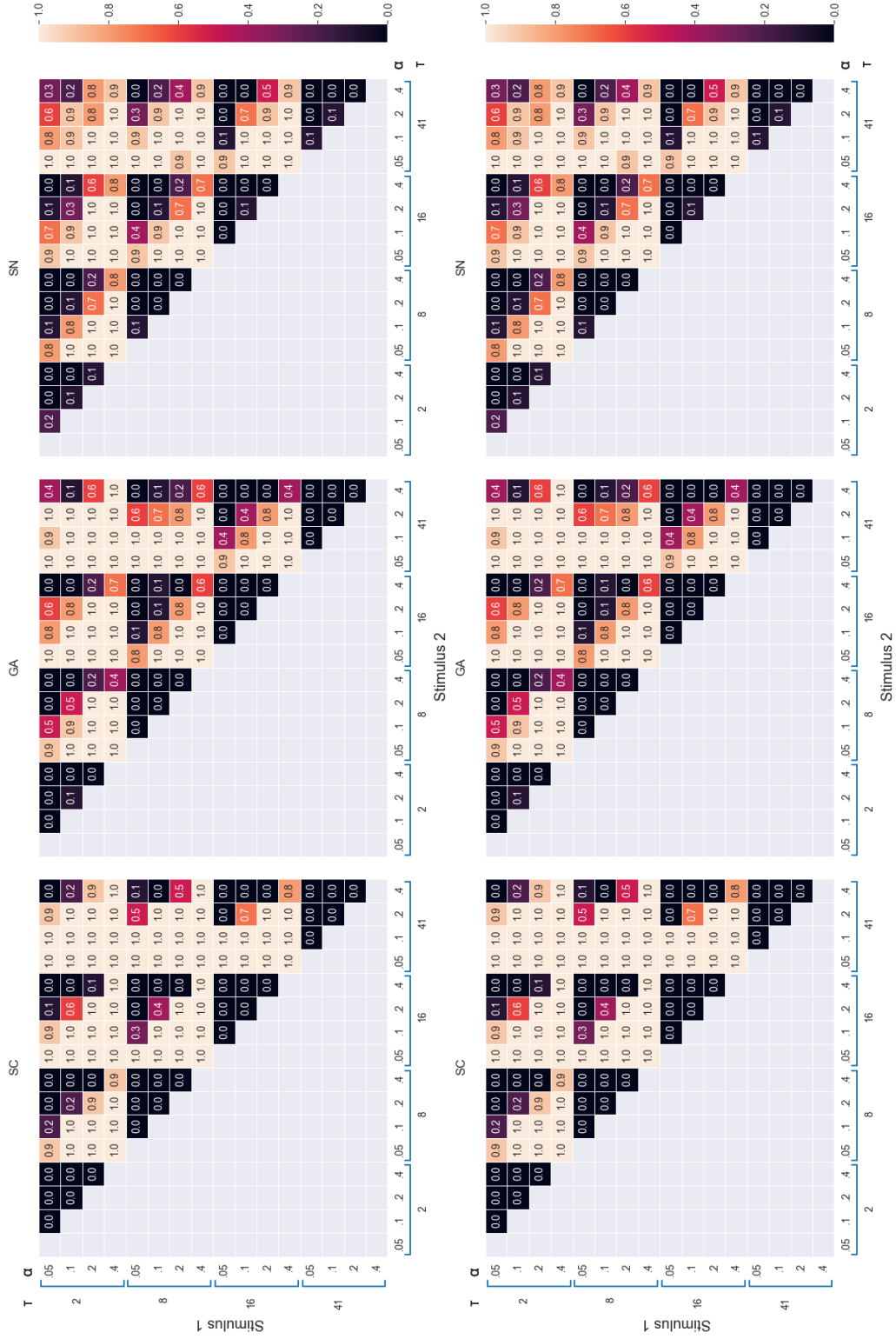


Figure 1: Heatmaps of the observers reflecting the decisions for all possible comparisons. The upper row displays the heatmaps of the first experiment (transparency perception) and the second row those of the second experiment (contrast perception). The numbers in each box indicate the likelihood of choosing Stimulus 1.

2 Observer Feedback Summary

Below, I list the key points summarizing the comments made by each observer after completing the experiments.

GA:

- Dark transparent media appeared different as if some effect was applied to the stimuli. Nevertheless, tried to focus solely on the transparency of the displayed stimuli.
- The experiments of this thesis were more challenging than those in the previous study.

SC:

- The transparency in dark, transparent media appeared clearer.
- Used very dark or very bright checks to make decisions when uncertain.
- The second experiment was more challenging than the first experiment.

SN:

- Has frequently based the decision on hard edges, the brightness of checks, or the color difference of neighboring checks.
- Perceived the checkerboard to be positioned in front of the transparent layer for some of the stimuli with the highest transmittance.